

https://doi.org/10.1070/QEL18057

Rubidium frequency standard with pulsed optical pumping and frequency instability of $2.5\times10^{-13}\tau^{-1/2}$

V.N. Baryshev, G.V. Osipenko, A.V. Novoselov, A.G. Sukhoverskaya, A.I. Boyko, M.S. Aleynikov

Abstract. **The work is dedicated to the further development of a compact quantum frequency standard based on a rubidium gas cell with a mixture of buffer gases. The results of frequency measurements and analysis of short-term frequency instability obtained on a laboratory prototype of a microwave rubidium atomic frequency standard (RAFS) with pulsed optical pumping (POP) are presented. The main in magnitude contributions to the overall frequency instability of the RAFS with POP are estimated. Short-term frequency instability expressed in terms of the Allan deviation and measured at averaging times τ up to several tens of seconds, $\sigma_y(\tau) = 2.5\times10^{-13}\tau^{-1/2}$, coincides satisfactorily with the calculated value of $\sigma_y(\tau) = 2.1\times10^{-13}\tau^{-1/2}$.**

Keywords: *quantum frequency standard on a rubidium gas cell, pulsed optical pumping, Ramsey microwave excitation scheme, diode laser, frequency modulation spectroscopy, acousto-optic modulator.*

1. Introduction

The rapid development of new technologies related to the use of positioning and synchronisation signals provided by global navigation satellite systems (GNSS) required a reduction to submetre values of uncertainty in determining the pseudorange calculated by the time delay between the moments of transmission and reception of satellite signals. The determination of the pseudorange with a sub-metre uncertainty requires maintaining the uncertainty level of the onboard time scale less than 1 ns during the day, which means that the onboard frequency standard should have a relative frequency instability in the region below the level of 1×10^{-14} with a daily averaging time of $\tau \sim 10^5$ s [1]. Rubidium frequency standards based on a gas cell with lamp optical pumping, satisfying this requirement for daily frequency instability, are currently most widely used as onboard clocks in satellite navigation systems. For example, the RAFS used on board the GNSS GPS Block IIF (USA) and BeiDou III (China) satellites have a short-term frequency instability expressed in terms of the Allan deviation of $\sim1\times10^{-12}\tau^{-1/2}$ and $6\times10^{-13}\tau^{-1/2}$, respectively, and their long-term daily frequency instability expressed in terms of the Hadamard deviation reaches $\sim3\times10^{-15}$ and 4×10^{-15}, respectively [2, 3]. The latter (Hadamard deviation) is insensitive to time-linear frequency drift, which makes it especially useful in analysing long-term RAFS frequency instability in the region of $\tau > 10^4$ s, where the frequency instability is no longer determined by white frequency noise proportional to $\tau^{-1/2}$, but usually takes the form of a linear frequency drift proportional to τ [4].

In frequency standards on gas cells with a buffer gas and continuous lamp optical pumping, this long-term drift of the clock transition frequency is determined by its temperature dependence and by the instability of the light frequency shift as well. In order to improve the frequency stability by significantly reducing the light shift, about 15 years ago, a technique of pulsed optical pumping (POP) in RAFS on a gas cell with a buffer gas, based on laser and digital technologies, was proposed and implemented [5].The POP technique is based on the time separation of three RAFS working phases: optical pumping, pulsed microwave interrogation according to the Ramsey scheme, and optical detection. Thus, the microwave clock transition occurs when there is no laser radiation in the cell, which leads to a significant light shift suppression. Pulsed microwave interrogation according to the Ramsey scheme allows obtaining narrow (150–200 Hz) Ramsey fringes with a central fringe contrast exceeding 40% [5, 6]. The signal-to-noise ratio of the optically detected clock signal in RAFS with POP can be several tens of thousands, making the level of short-term instability of several units $10^{-13}\tau^{-1/2}$ practically achievable, which is unprecedented for lamp-pumped RAFS [1, 5]. The record value of instability, $1.7\times10^{-13}\tau^{-1/2}$, was obtained on the prototype of RAFS with POP presented 10 years ago in [5]. Such a low level of short-term instability, in turn, makes it possible to achieve, in the limit of white frequency noise, an instability level of several units of 10^{-15} already at averaging intervals of $\tau \sim 10^4$ s.

This work presents the results of frequency measurements and analysis of short-term frequency instability obtained on a laboratory prototype of a microwave rubidium frequency standard with POP, presented for the first time in [6]. The main contributions to the overall instability of the RAFS frequency, introduced by the shot noise of the photodetection process, photodetector noise, laser noise, and phase noise of the microwave frequency synthesiser, are estimated.

2. Experimental setup and results

The technique of POP and pulsed microwave excitation according to the Ramsey scheme allows obtaining a clock signal with a narrow linewidth, which is insensitive to power variations in the interrogation microwave signal and laser radiation inten-

V.N. Baryshev, G.V. Osipenko, A.V. Novoselov, A.G. Sukhoverskaya, A.I. Boyko, M.S. Aleynikov All-Russian Scientific Research Institute for Physical-Engineering and Radiotechnical Metrology (VNIIFTRI), pos. Mendeleevo, Solnechnogorsk, 141570 Moscow region, Russia; e-mail: baryshev@vniiftri.ru

Received 22 March 2022; revision received 27 April 2022
Kvantovaya Elektronika **52** (6) 538–543 (2022)
Translated by M.A. Monastyrskiy

sity variations, and depends only on the duration of the interval between microwave field pulses – Ramsey time T_R. The full width at half maximum of the Ramsey central fringe is $\Delta\nu_{1/2} = 1/(2T_R)$. Figure 1 shows the time sequence of pump pulses t_p, microwave pulses t_1, and detection pulses t_{det} (T_c is the duration of a single frequency measurement cycle).

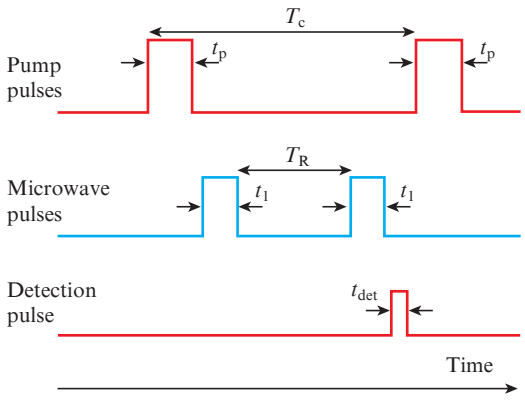

Figure 1. (Colour online) Time sequence of optical pumping pulses t_p, microwave pulses t_1, and detection pulse t_{det} (T_R is the Ramsey time, T_c is the duration of one frequency measurement cycle).

The experimental scheme (Fig. 2) of the laboratory prototype of RAFS with POP includes: 1) a physical part containing an ^{87}Rb cell with a mixture of Ar–N_2 buffer gases, placed in a cylindrical microwave resonator; 2) a laser system generating radiation at a wavelength of the D_2 absorption line of the Rb atom, with a structural unit for saturated absorption spectroscopy in the reference Rb cell (Fig. 3) and with an acousto-optic modulator (AOM) that performs the functions of a frequency shifter and an optical pulse generator; and 3) a system for generating a microwave signal at a frequency of 6.834 GHz and a digital control system that generates all optical and electrical signals of the prototype, including the error signal for automatic frequency tuning of the quartz oscillator.

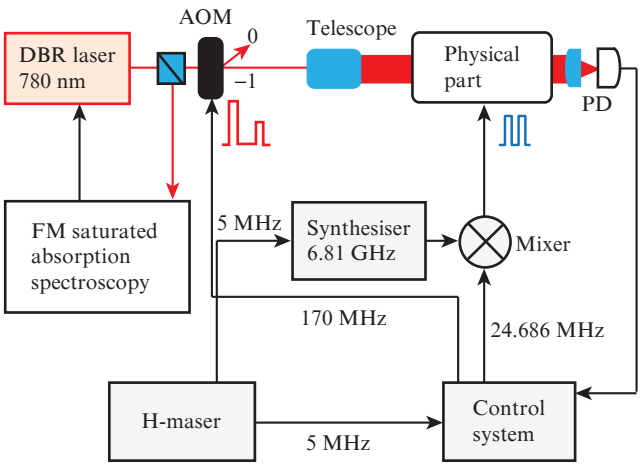

Figure 2. (Colour online) Experimental scheme of RAFS with POP: (AOM) acoustooptic modulator in anisotropic Bragg diffraction regime; (PD) photodetector; (DBR) laser with distributed Bragg reflection.

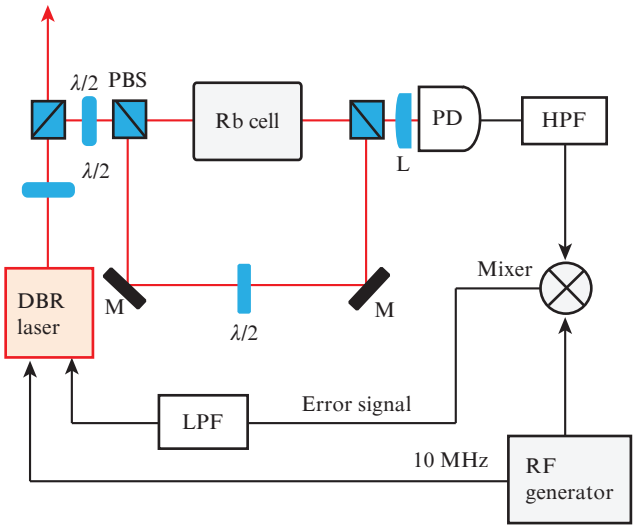

Figure 3. (Colour online) Schematic of the saturated absorption frequency–modulation spectroscopy unit:
(PBS) polarising beam splitter; (L) lens; (HPF, LPF) high- and low-pass filters; (PD) photodetector; (M) mirror; (λ/2) half-wave plate.

In the absence of a light frequency shift in RAFS with POP, its temperature sensitivity has a decisive influence on the mid- and long-term frequency instability. Long-term stability of the cell temperature at a level of ~100 μK is necessary to maintain the long-term instability of the RAFS frequency in the region below 10^{-14} at averaging times $\tau \sim 10^4 - 10^5$ s [1, 5, 7].

In our prototype, a ^{87}Rb cell with a diameter of 56 mm and a length of 58 mm, placed in a cylindrical cavity with TE_{011} mode and a moderate (about 300) Q-factor, contained a two-component mixture of Ar–N_2 buffer gases at a total pressure of 25 Torr and partial pressure ratio $P_{Ar}/P_{N_2} = 2$. A cavity with a cell filling almost its entire internal volume is located inside a solenoid, which creates a magnetic field directed along the cavity axis to eliminate degeneracy in magnetic quantum states. The Zeeman frequency f_Z corresponding to the Zeeman shift of the magnetic sublevels was ~16 kHz. The physical part of the laboratory prototype was shielded from external magnetic fields and thermally stabilised with an accuracy of about several mK using a two-stage temperature control system. The laser beam diameter, as in work [6], was equal to 10 mm.

Figure 4 shows the temperature dependence of the frequency of the RAFS with POP. The inversion point of this dependence (or the temperature compensation point) is reached at the temperature $T = 32.6$ °C with a linear approximation of the dependence $\delta\nu/\delta T \approx 2.9 \times 10^{-12}$ Hz K^{-1}. Note that in the cell with a mixture of Ar–Ne buffer gases used in [6], we did not reach the inversion point and observed a linear temperature dependence of the frequency up to the limit determined by the parameters of the internal stage of the thermostatic system, $T \sim 65$ °C. Actually, this explains the decision to replace the cell with a mixture of Ar–Ne buffer gases by a cell with Ar–N_2 buffer gases.

Figure 5 shows a Ramsey line with the central fringe linewidth $\Delta\nu_{1/2} = 151$ Hz and contrast $C = 31\%$, obtained in a cell with Ar–N_2 buffer gases at a temperature of about 32.6°C (the inversion points of the temperature dependence of the frequency) and when sweeping the microwave synthesiser frequency relative to the clock transition frequency of 6.834682610 GHz.

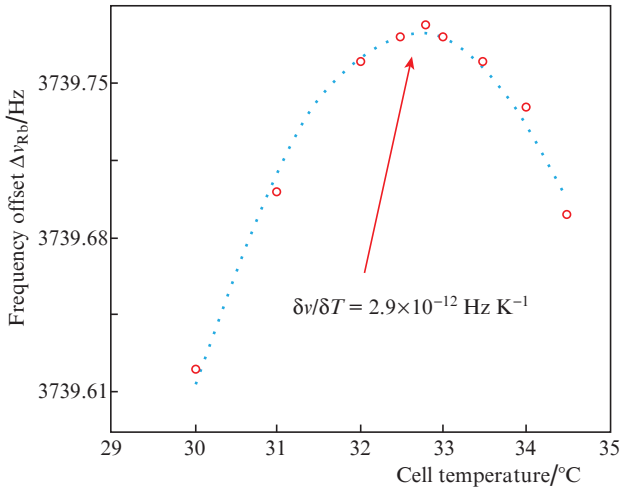

Figure 4. (Colour online) Temperature dependence of the clock transition frequency of RAFS with POP.

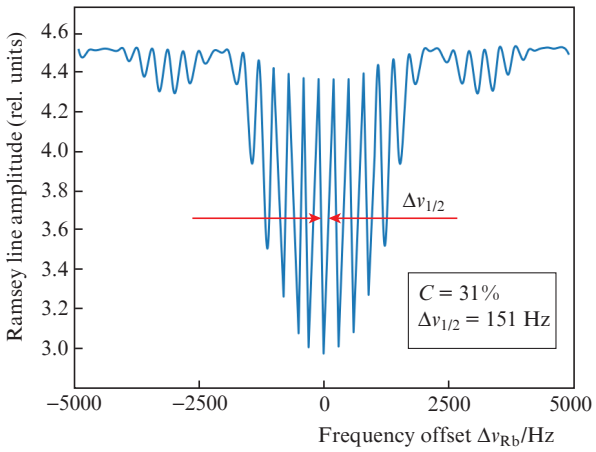

Figure 5. (Colour online) Ramsey line with central fringe linewidth $\Delta\nu_{1/2}$ = 151 Hz and contrast C = 31%, obtained in the Rb cell with Ar–N_2 buffer gases at a temperature T = 32.6 °C and when sweeping the microwave synthesiser frequency relative to the clock transition frequency of 6.834682610 GHz.

In this prototype of RAFS with POP, the Ramsey line is optimised for contrast and linewidth at the following parameters: pump pulse duration t_p = 0.3 ms, microwave pulse duration t_1 = 0.45 ms, and detection pulse duration t_{det} = 0.15 ms; the time between the end of the first microwave pulse and the beginning of the second is T_R = 3.3 ms. The full cycle duration is T_c = 4.791 ms, including some pauses between optical and microwave pulses. The cycle repetition rate is $f_c = 1/T_c \approx 208.7$ Hz, and the Q-factor of the line is $Q_{line} \approx 4.5\times10^7$. These parameters are used in the presented below calculations and measurements of the main noise contributions to the overall short-term instability of the laboratory prototype of RAFS with POP.

As in work [6], we used a laser diode with distributed Bragg reflection (DBR) and a radiation spectrum linewidth of less than 1 MHz. The laser provided an output radiation power of 80 mW at a wavelength of 780.24 nm, which was sufficient for frequency-modulation spectroscopy of saturated absorption in a ^{87}Rb reference cell, the formation of optical pump and detection pulses, and also for spatial filtering radiation, realised by insertion of the laser light into a single-mode polarisation-maintaining fibre-optic cable. The choice of the absorption line D_2 (λ = 780.24 nm) of the ^{87}Rb isotope for pumping and detection in RAFS with POP is substantiated in detailed theoretical studies presented in [5].

The injection current of the DBR laser was modulated by a sinusoidal signal at a frequency of ~10 MHz. Both beams (saturating and probing) were modulated at this frequency. The beat signal from the photodetector was mixed in a mixer with a 10 MHz signal from the RF generator, and the output signal of the dispersion-like mixer was used as an error signal in the feedback loop of the laser injection current. The laser frequency was locked to the cross-over resonance $F = 2 \leftrightarrow F' = 2 - F = 2 \leftrightarrow F' = 3$ of the D_2 absorption line of the ^{87}Rb atom (here, F and F' are the total angular momenta of the atom in the ground and excited states, respectively). This resonance was chosen to stabilise the laser frequency in the process of optimising the Ramsey line contrast in the working cell by frequency locking to various saturated absorption resonances in the reference cell. The laser radiation frequency was shifted by –170 MHz from the frequency of the resonance $F = 2 \leftrightarrow F' = 2 - F = 2 \leftrightarrow F' = 3$ after a single passage of radiation through an acousto-optic modulator developed at the VNIIFTRI, operating in the anisotropic Bragg regime and performing the functions of a frequency shifter and an optical pulse generator [6, 8]. Then the diffracted beam (–1st order of diffraction) was inserted into a single-mode polarisation-maintaining fibre cable (not shown in Fig. 2), which fed the radiation to the physical part of the setup. In order to avoid the influence of external temperature fluctuations on the polarisation state of the radiation emerging from the cable, special attention was paid to achieving an exact coincidence of the direction of linearly polarised radiation entering the cable and the direction of one of its optical axes. All optical, fibre-optic and optoelectronic elements of the laser system, including the AOM, which, like the fibre-optic cable, has birefringent properties, were not thermally stabilised and were freely placed on an open optical table.

Let us consider the main noise sources contributing to the overall short-term frequency instability of RAFS with POP, which in terms of the Allan deviation is expressed as

$$\sigma_y = \sqrt{(\sigma_y^{sn})^2 + (\sigma_y^{Dick})^2 + (\sigma_y^{AM})^2 + (\sigma_y^{PD})^2}, \quad (1)$$

where σ_y^{sn} is the instability associated with the shot noise of the photodetection process; σ_y^{Dick} the instability associated with the phase noise of the synthesiser signal at a frequency of 6.8 GHz (the noise is transferred to the clock signal via the Dick effect); σ_y^{AM} is the instability associated with the amplitude noise of the laser; and σ_y^{PD} is the instability associated with the intrinsic noise of the photodetector.

The shot noise associated with the process of photodetection of the clock signal sets the theoretical limit of frequency stability and can be calculated as follows [5]:

$$\sigma_y^{sn}(\tau) = \frac{\sqrt{T_c}}{\pi Q_{line} R_{SN}} \tau^{-1/2}. \quad (2)$$

Here the Q-factor of the line is

$$Q_{line} = \frac{\nu_{Rb}}{\Delta\nu_{1/2}}; \quad (3)$$

ν_{Rb} is the clock transition frequency in the ^{87}Rb atom; $\Delta\nu_{1/2}$ is the linewidth of the atomic resonance line; and R_{SN} is the signal-to-noise ratio, which can be written as [5]

$$R_{SN} = C\sqrt{\eta_q N_F}, \tag{4}$$

where C is the central fringe contrast of the resulting Ramsey line; η_q is the quantum efficiency of the photodetector; N_F is the number of photons reaching the photodetector,

$$N_F = \frac{P_0\lambda}{hc}t_d; \tag{5}$$

P_0 and λ are the power and wavelength of radiation; h is Planck's constant; c is the speed of light; and t_d is the duration of the optical detection phase. At $C = 31\,\%$, the quantum efficiency of the photodetector $\eta_q = 0.8$, the number of photons $N_F \approx 2.9\times10^{10}$, the radiation power incident on the photodetector $P_0 = 0.049$ mW, the radiation wavelength $\lambda = 780$ nm, and the duration of the optical detection phase $t_d = 0.15$ ms, the theoretical limit of instability is $\sigma_y^{sn}(\tau) = 2\times10^{-14}\tau^{-1/2}$.

In quantum frequency standards operating in pulsed regime, in particular, when operating according to the Ramsey scheme, the phase noise of the microwave signal worsens the frequency stability due to a phenomenon known as the Dick effect [9, 10]. For microwave π/2 pulses, this noise is expressed as [5]

$$\sigma_y^{Dick}(\tau) = \left(\sum_{k=1}^{\infty}\mathrm{sinc}^2\left(k\pi\frac{T_R}{T_c}\right)S_y^{Dick}(kf_c)\right)^{1/2}\tau^{-1/2}, \tag{6}$$

where $S_y^{Dick}(f)$ is the power spectral density (PSD) of the phase noise of the microwave signal. Substituting into formula (6) the cycle repetition frequency $f_c \approx 208.7$ Hz, as well as the value of the measured PSD of the phase noise of the microwave signal at a frequency of 6.8 GHz (Fig. 6), we calculated the contribution of the phase noise of the frequency synthesiser (the Dick effect) to the short-term frequency instability: $\sigma_y^{Dick}(\tau) = 1.9\times10^{-13}\tau^{-1/2}$.

Another effect limiting the short-term stability of a quantum frequency standard (QFS) with POP in optical detection regime is the amplitude noise of the laser. The contribution of the noise of optical detection signals to the short-term frequency instability of the QFS with POP can be expressed using the well-known expression for the clock instability during periodic operation [5, 11, 12]:

$$\sigma_y^{AM}(\tau) = \frac{1}{\pi C Q_{line}}$$

$$\times\left(\sum_{n=1}^{\infty}\mathrm{sinc}^2(\pi n f_c t_{det})S_{RIN}^{AM}(nf_c)\right)^{1/2}\sqrt{\frac{T_c}{t_{det}}}\tau^{-1/2}, \tag{7}$$

where $S_{RIN}^{AM}(f)$ is the power spectral density of the relative intensity noise (RIN) of the detection signal.

The relative intensity noise measured during the detection pulse action consists of the amplitude noise of the laser and the frequency noise of the radiation converted into amplitude fluctuations. It describes fluctuations in the laser optical power, which are mainly due to intrinsic optical phase and frequency fluctuations caused by spontaneous radiation.

To estimate the contribution of the laser amplitude noise to instability, we performed a spectral Fourier analysis of the signals from the photodetector, recorded both when the laser radiation frequency was locked and in the absence of radiation, sending these signals to a digital oscilloscope operating in the FFT (fast Fourier transform) regime. When recording FFT signals, the resolution bandwidth was 1 Hz, and the frequency range was 100 Hz–3 kHz. The resulting PSD dependence shown in Fig. 7 was approximated by the function $S_{RIN}^{AM}(f) = A\ \mathrm{Hz}^{-1} + B/f + C\ \mathrm{Hz}/f^2$ using the least

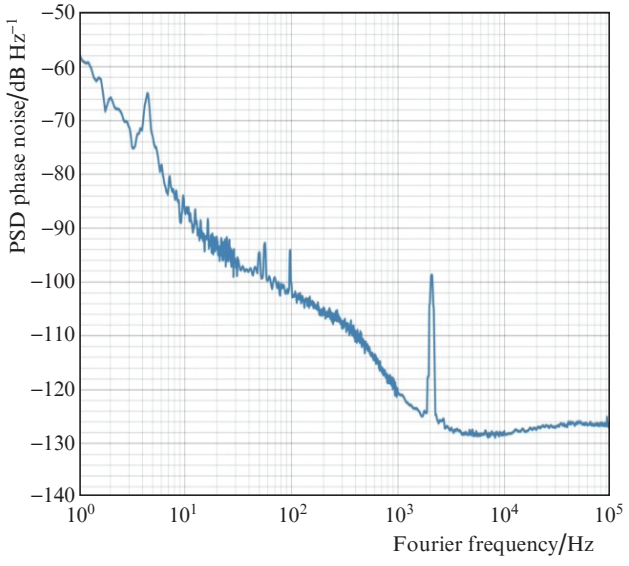

Figure 6. (Colour online) Power spectral density of phase noise of the microwave signal at a frequency of 6.8 GHz.

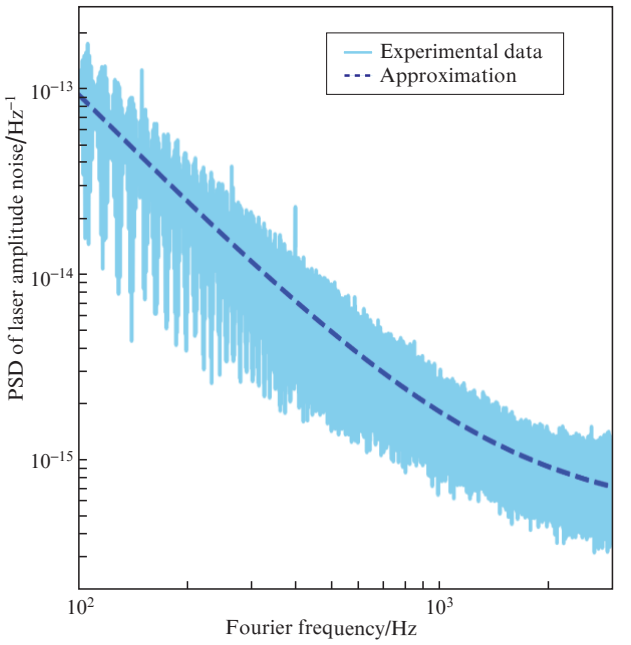

Figure 7. (Colour online) Power spectral density of the amplitude noises of the DBR laser.

squares method. Then, the PSD RIN values corresponding to certain harmonics of the cycle frequency f_c were calculated, on the basis of which, using formula (7), the contribution of laser noise to the short-term frequency instability was determined for the optimal parameters of the RAFS prototype with POP. The contribution of the amplitude noise of the probing detecting radiation, which forms the clock signal, to the overall instability was $\sigma_y^{\mathrm{AM}}(\tau) = 2.8 \times 10^{-14}\tau^{-1/2}$.

Similarly, the contribution of the photodetector's intrinsic noise, which introduces additive white frequency noise, was evaluated. Measurements carried out in the absence of laser radiation showed that $\sigma_y^{\mathrm{PD}}(\tau) = 7.5 \times 10^{-14}\tau^{-1/2}$.

As a result, the total contribution determining the theoretical value of the overall frequency instability of our prototype is $\sigma_y(\tau) = 2.1 \times 10^{-13}\tau^{-1/2}$ (Table 1).

Table 1. Noise sources and corresponding contribution to frequency instability.

Noise sources	$\sigma_y(\tau)$
Shot noise limit	$2 \times 10^{-14}\tau^{-1/2}$
Dick effect	$1.9 \times 10^{-13}\tau^{-1/2}$
Laser noise	$2.8 \times 10^{-14}\tau^{-1/2}$
Photodetector noise	$7.5 \times 10^{-14}\tau^{-1/2}$
Overall instability $\sqrt{\Sigma_i \sigma_{y_i}^2}$	$2.1 \times 10^{-13}\tau^{-1/2}$

Figure 8 shows the time dependence of short-term instability (Allan deviation) obtained as a result of frequency measurements on our laboratory prototype in a cell with a mixture of $Ar-N_2$ buffer gases at a total pressure of 25 Torr and the partial pressure ratio $P_{Ar}/P_{N_2} = 2$ with the optimal parameters mentioned above. Up to the averaging time $\tau = 20$ s, the typical $\tau^{-1/2}$ dependence inherent in white frequency noise is clearly observed. The Allan deviation at $\tau = 1$ s is 2.5×10^{-13}, which is in satisfactory agreement with the previously calculated value of 2.1×10^{-13}. The stability degradation, which begins at averaging times exceeding $\tau = 20$ s, is explained by the inertia of the feedback loops of the RAFS temperature control system, which reacts to periodic temperature changes inside the laboratory room caused by the air conditioning system. In Fig. 9, this temperature sensitivity to fluctuations in the external temperature is clearly manifested at averaging times in a wide range around the value $\tau = 300$ s, which corresponds to the peak of instability. The Allan deviation reaches a minimum value of 4.4×10^{-14} at $\tau = 5000$ s, after which its behaviour takes the form of a frequency drift. External impact on the frequency stability of RAFS with POP due to changes in room temperature also leads to a deterioration of the short-term stability to 33.5×10^{-13} at $\tau = 1$ s (Fig. 9).

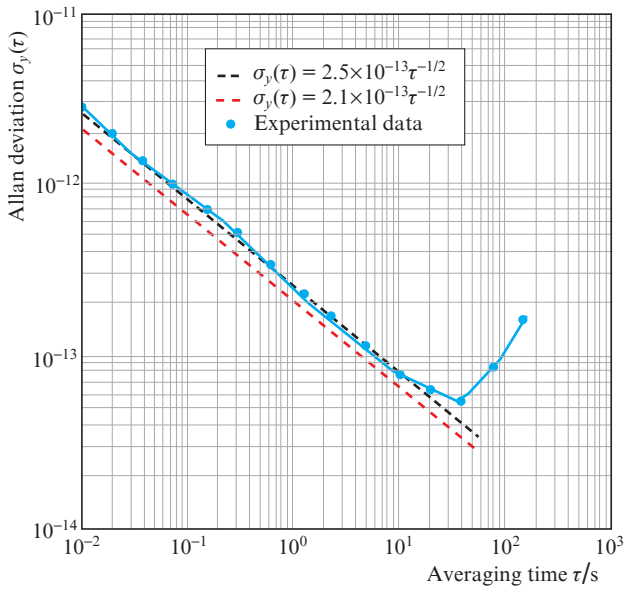

Figure 8. (Colour online) Measured short-term instability of RAFS with POP in the form of Allan deviation relative to the frequency of the active H oscillator.

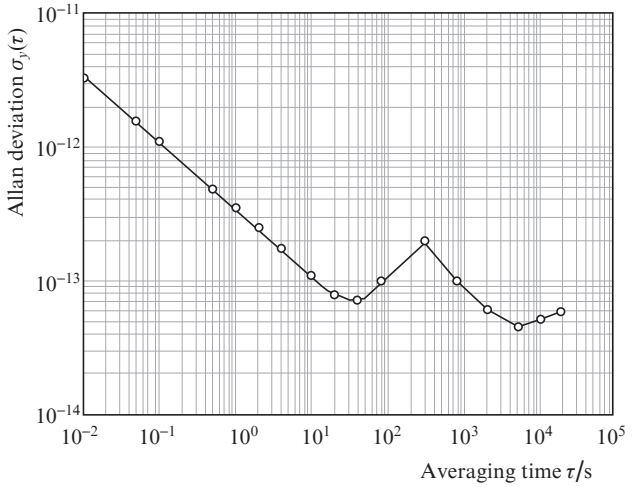

Figure 9. Measured long-term instability of RAFS with POP in the form of Allan deviation relative to the frequency of the active H maser.

3. Conclusions

The results of frequency measurements and analysis of short-term frequency instability obtained on a laboratory prototype of a microwave rubidium frequency standard using the pulsed optical pumping technique are presented. The main contributions in terms of magnitude to the overall frequency instability of RAFS with POP are estimated. Expressed in terms of the Allan deviation and measured at averaging times τ up to several tens of seconds, the short-term frequency instability $\sigma_y(\tau) = 2.5 \times 10^{-13}\tau^{-1/2}$ satisfactorily coincides with the calculated instability value $\sigma_y(\tau) = 2.1 \times 10^{-13}\tau^{-1/2}$.

The currently attained level of temperature sensitivity of the prototype frequency hinders the achievement of frequency instability below 1×10^{-14} at averaging times of $10^4 - 10^5$ s. We believe that our current work on miniaturising the design of the RAFS prototype with POP, primarily by replacing the cylindrical microwave cavity with a noticeably smaller magnetron-type cavity (Fig. 10), will entail a significant reduction in the weight and size parameters of the physical part and temperature sensitivity of the frequency of the RAFS prototype with POP as a whole.

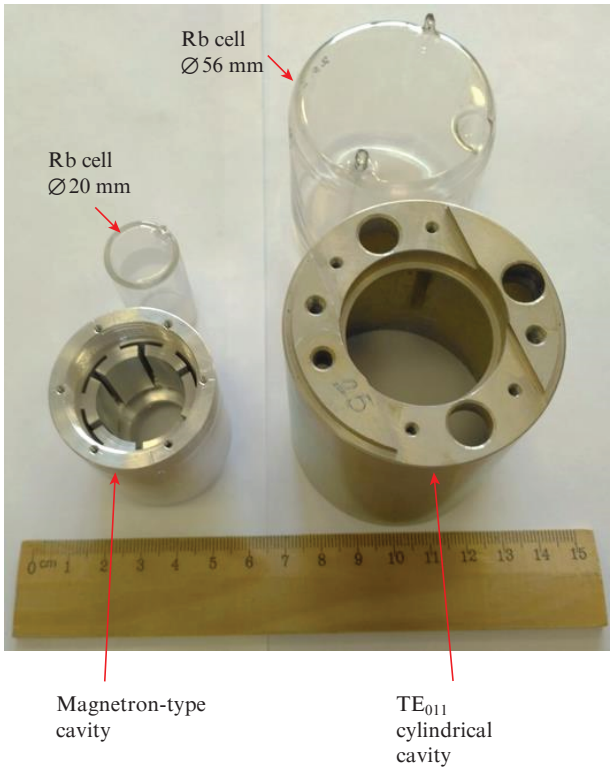

Figure 10. (Colour online) Photograph of the cylindrical microwave resonator and Rb cell (∅56 mm) used in this work (right), and a noticeably smaller magnetron-type resonator and Rb cell (∅20 mm) (left) to be used in subsequent works.

References

1. Micalizio S., Levi F., Calosso C.E., Gozzelino M. *GPS Solutions*, **25** (3), 94 (2021). DOI: 10.1007/s10291-021-01136-9.
2. Vannicola F., Beard R., White J., Senior K., Largay M., Buisson J.A. *Proc. 42nd Annual Precise Time and Time Interval (PTTI) Systems and Applications Meeting* (Reston, Virginia, 2010) pp 181–196.
3. Ganghua Mei, Da Zhong, Shaofeng An, Feng Zhao, Feng Qi, Fang Wang, Gang Ming, Wenbin Li, Pengfei Wang. *Proc. 2016 30th European Frequency and Time Forum (EFTF)* (York, UK, 2016); http://doi.org/10.1109/eftf.2016.7477803:1-4.
4. Riley W.J. *Handbook of Frequency Stability Analysis* (NIST Spec. Publ. 1065, 2008) p. 20.
5. Micalizio S., Calosso C., Godone A., Levi F. *Metrologia*, **49**, 425 (2012).
6. Baryshev V.N., Aleinikov M.S., Osipenko G.V., Blinov I.Yu. *Quantum Electron.*, **48** (5), 443 (2018) [*Kvantovaya Elektron.*, **48** (5), 443 (2018)].
7. Calosso C.E., Godone A., Levi F., Micalizio S. *IEEE Trans. Ultrason. Ferroelect. Freq. Control*, **59** (12), 2646 (2012).
8. Epikhin V.M., Baryshev V.N., Slyusarev S.N., Aprelev A.V., Blinov I.Yu. *Quantum Electron.*, **49** (9), 857 (2019) [*Kvantovaya Elektron.*, **49** (9), 857 (2019)].
9. Santarelli G., Audoin C., Makdissi A., Laurent P., Dick G.J., Clairon A. *IEEE Trans. Ultrason. Ferroelect. Freq. Control*, **45** (4), 887 (1998).
10. Dick G.J., Prestage J.D., Greenhall C.A., Maleki L. *Proc. of the 22th Annual Precise Time and Time Interval Systems and Applications Meeting* (Vienna, Virginia, 1990) pp 487 – 508.
11. Riehle F. *Frequency Standards: Basics and Applications* (Weinheim: Wiley-VCH, 2006; Moscow: Fizmatlit, 2009).
12. Kang S. Gharavipour M., Affolderbach C., Mileti G. *Electron. Lett.*, **51** (22), 1767 (2015).